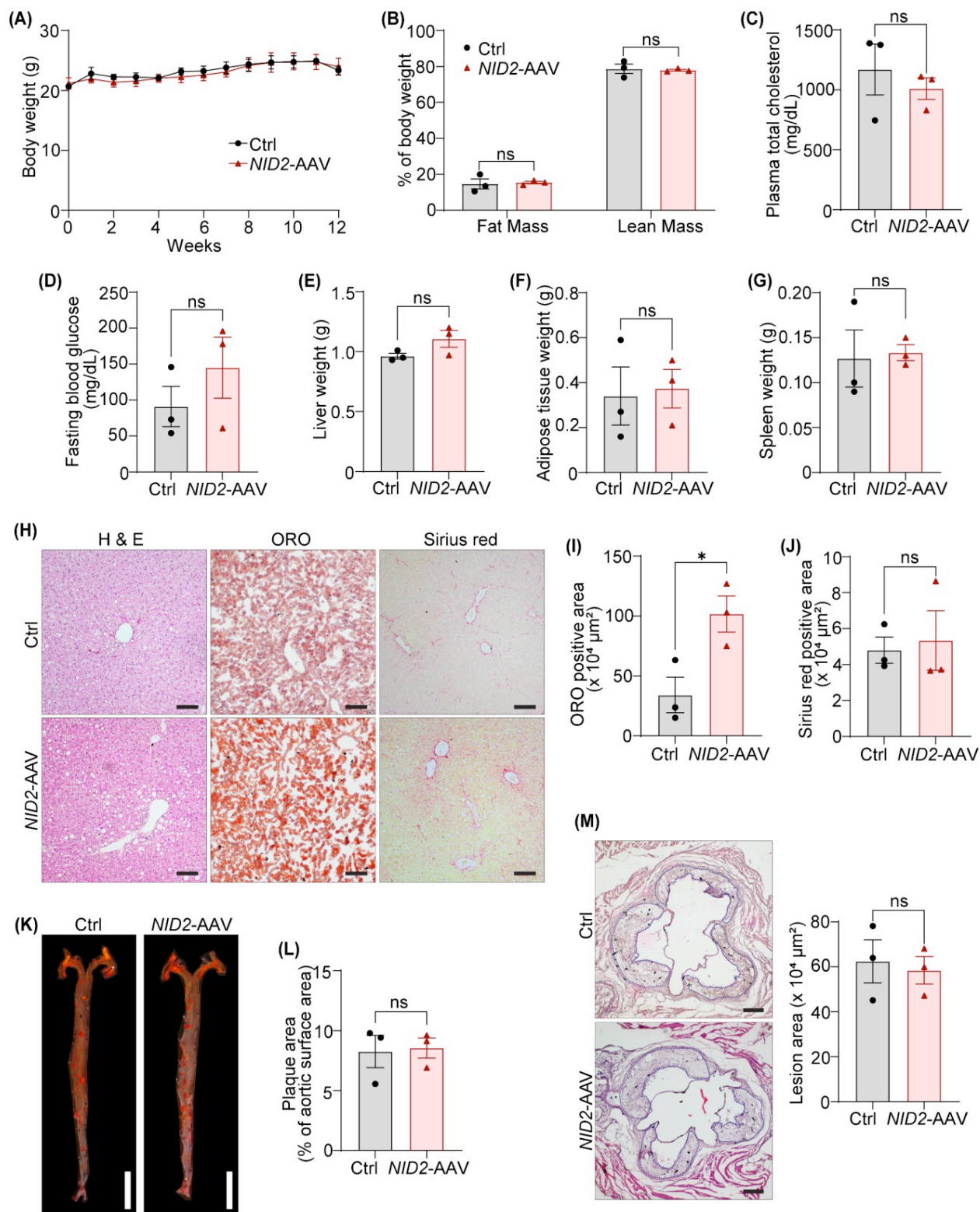


### Supplementary Materials

**Table S1:** List of primers used for mRNA quantitation using quantitative real-time PCR.

<b>Gene name</b>	<b>Primer sequences</b>
Human <i>NID2</i>	F: 5'-TAG GCG CTT ACG AGG AGG TCAA A-3'
	R: 5'-TAT CAG ACC CAT CAG ATG CCA AAA C-3'
Mouse <i>Nos2</i>	F: 5'-GTT CTC AGC CCA ACA ATA CAA GA-3'
	R: 5'-GTG GAC GGG TCG ATG TCA C-3'
Mouse <i>Tnfa</i>	F: 5'-TCC CAG GTT CTC TTC AAG GGA-3'
	R: 5'-GGT GAG GAG CAC GTA GTC GG-3'
Mouse <i>Ldlr</i>	F: 5'-ACC TGC CGA CCT GAT GAA TTC-3'
	R: 5'-GCA GTC ATG TTC ACG GTC ACA-3'
Mouse <i>Il6</i>	F: 5'-CAC AAG TCG GAG GCT TAA T-3'
	R: 5'-GTG CAT CAT CGT TCG TCA TAC-3'
Mouse <i>Cd36</i>	F: 5'-ATG GGC TGT GAT CGG AAC TG-3'
	R: 5'-TTT GCC ACG TCA TCT GGG TTT-3'
Mouse <i>Msr1</i>	F: 5'-CTG GAC TGA CGA AAT CAA GGA A-3'
	R: 5'-TGG AGG AGA GAA TCG AAA GCA-3'
Mouse <i>Fasn</i>	F: 5'-TTC CAA GAC GAA AAT GAT GC-3'
	R: 5'-AAT TGT GGG ATC AGG AGA GC-3'
Mouse <i>Cpt1a</i>	F: 5'-ACC ACT GGC CGC ATG TCA AG-3'
	R: 5'-CAG CGA GTA GCG CAT AGT CA-3'
Mouse <i>Gapdh</i>	F: 5'-AGG TCG GTG TGA ACG GAT TTG-3'
	R: 5'-GGG GTC GTT GAT GGC AAC A-3'



**Figure S1: NID2 overexpression in females elevates hepatic lipid accumulation.** Female *Apoe<sup>-/-</sup>* mice were injected with control and NID2-AAV intraperitoneally, fed a Western diet for 12 weeks, and analyzed. **(A - G)** Bar diagrams represent body weight

**(A)**, whole-body fat mass and lean mass **(B)**, plasma total cholesterol **(C)**, fasting blood glucose **(D)**, liver weight **(E)**, adipose tissue weight **(F)** and spleen weight **(G)**. **(H)** Representative images of liver sections stained with H & E (lipid droplets), ORO (neutral lipid accumulation) and, Sirius red (fibrosis), scale bar 100  $\mu$ m. Bar diagrams represent lipid accumulation **(I)** and fibrosis area **(J)** in female mice. **(K)** Representative *en face* ORO staining of whole aortas, scale bar 5 mm. **(L)** Bar diagram represents ORO-positive areas in whole aortas. **(M)** Representative images of aortic root cross-sections stained with H & E, scale bar: 200  $\mu$ m. Bar diagram represents lesion area, ( $n = 3$ ). Statistical analyses were performed using a two-way ANOVA followed by Sidak post hoc test for multiple comparisons **(A)**, and a two-tailed unpaired t-test **(B - G, I, J, L and M)**. Data represent mean  $\pm$  SEM. \* $P < 0.05$ .

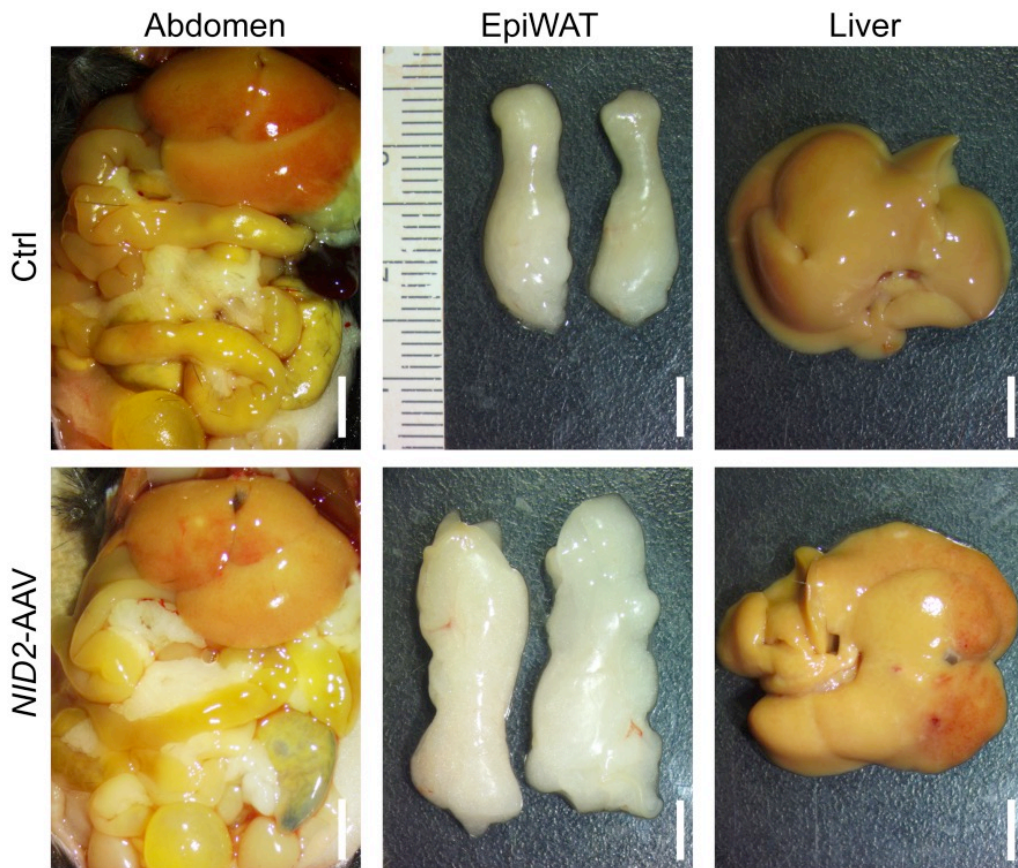


**Figure S2: Representative *in situ* images of the abdomen, epididymal white adipose tissue and liver of control and *NID2*-AAV-injected male mice.**

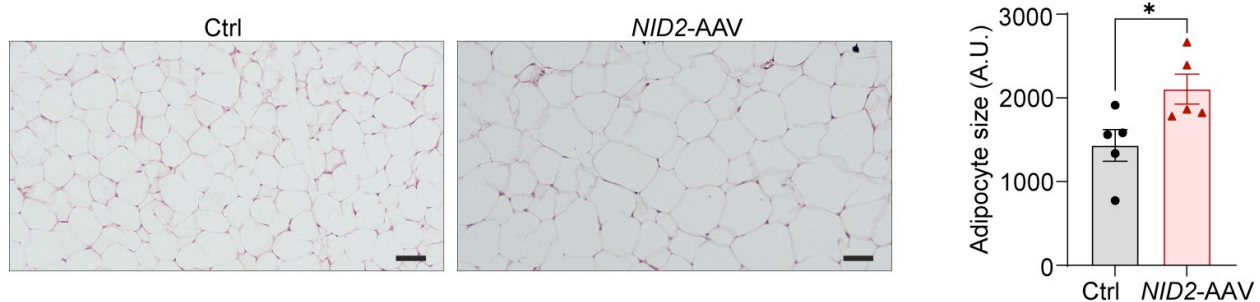


**Figure S3: *NID2* overexpression in male mice increases adipocyte size.**  
Representative images of EpiWAT sections stained with H & E, scale bar: 50  $\mu$ m. The bar diagram represents mean adipocyte size in male control and *NID2*-AAV-injected *Apoe*<sup>-/-</sup> mice. ( $n = 5$ ). Statistical analyses were performed using a two-tailed unpaired t-test. Data represent mean  $\pm$  SEM. \* $P < 0.05$ .

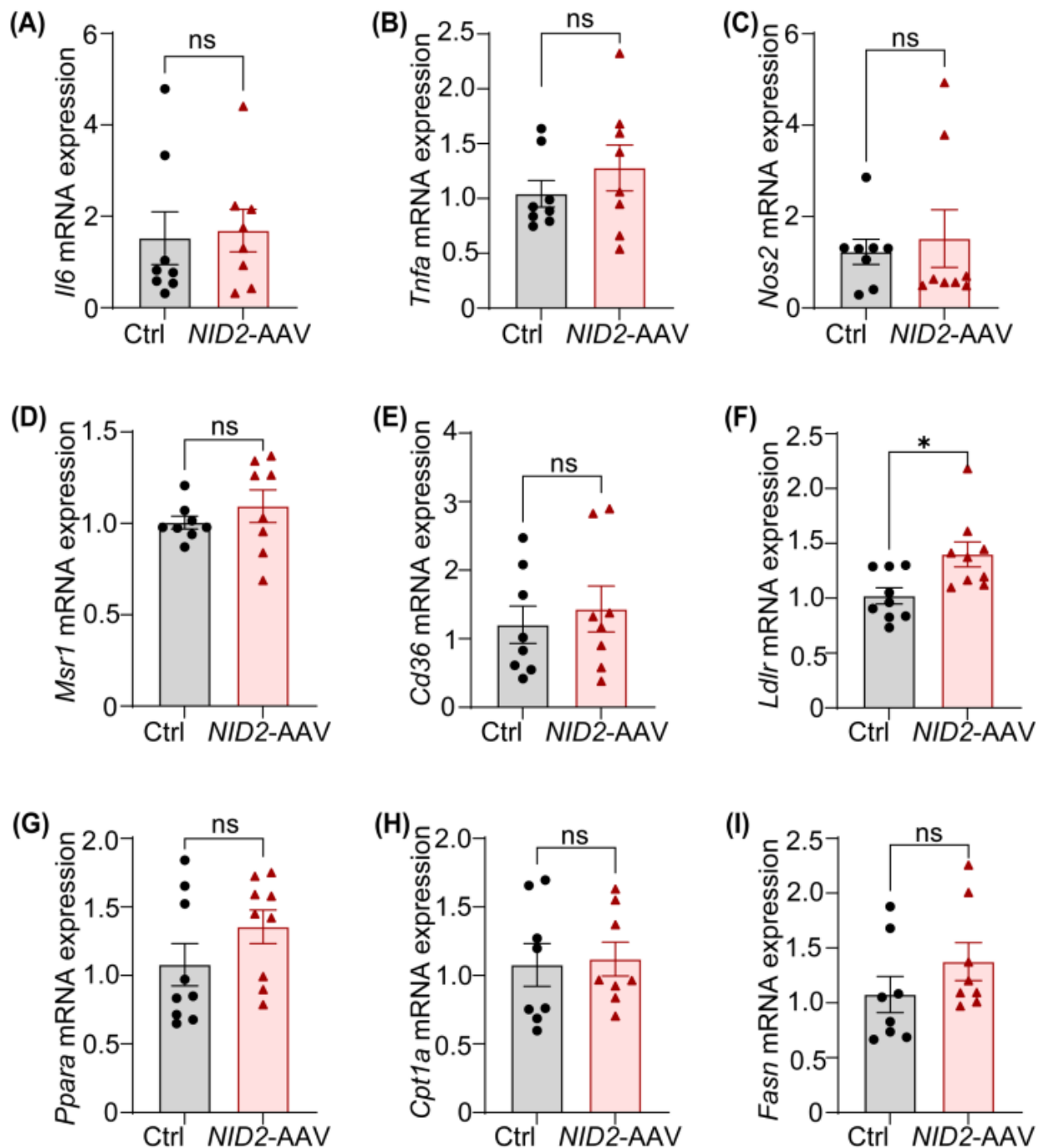


**Figure S4: Expression of various lipid metabolism-related genes in the livers of control and *NID2*-overexpressing mice. (A - I)** Bar diagrams represent relative mRNA expressions of various pro-inflammatory and lipid metabolism genes in the livers of control and *NID2*-AAV-injected mice using qRT-PCR, *Il6* (A), *Tnfa* (B), *Nos2* (C), *Msr1* (D), *Cd36* (E), *Ldlr* (F), *Ppara* (G), *Cpt1a* (H) and *Fasn* (I), ( $n = 8 - 9$ ). Statistical analyses were performed using a two-tailed unpaired Mann-Whitney test (A, C, E, F, and I) and a two-tailed unpaired t-test, (B, D, G and H). Data represent mean  $\pm$  SEM. \* $P < 0.05$ .